Acoustic detection and localisation system for *Hylotrupes bajulus* L. larvae using a MEMS microphone array

Roberto D. Martínez [a], Alberto Izquierdo [b], Juan José Villacorta [b], Lara del Val [b,*], Luis-Alfonso Basterra [c]

[a] *Department of Agricultural and Forestry Engineering, E.T.S.I Agrarias, University of Valladolid (Spain), Avenida de Madrid, 57, 34004 Palencia, Spain*
[b] *Department of Signal Theory and Communications and Telematic Engineering, ETSI Telecomunicación, University of Valladolid (Spain), Paseo Belén, 15, 47011 Valladolid, Spain*
[c] *Timber Structures and Wood Technology Research Group, ETS Arquitectura, University of Valladolid (Spain), Avenida de Salamanca, 18, 47014 Valladolid, Spain*

ARTICLE INFO

ABSTRACT

A novel system for acoustic detection of the presence of xylophagous insect larvae inside structural timber beams is presented. It is based on an extensive array of MEMS microphones that allows the acoustic detection and localisation of the larvae when they are active. In a first phase, the activity of the larvae is continuously detected by means of frequency filtering and a sliding energy estimator, and after that, a set of short-duration segmented signals is generated, which obtains the spatial localisation of the larvae, by means of a shaping algorithm based on delay-sum beamforming techniques.

The tests carried out demonstrate that it is possible to detect and locate multiple larvae of *Hylotrupes bajulus* L. inside structural-sized pieces of wood of *Pinus sylvestris* L., as well as their internal trajectory.

In the future, the system could address the identification of the specific type of xylophage responsible for the deterioration by using machine learning or equivalent techniques, based on the temporal and frequency information of the detected sound events.

The aim of this work is to control unintentional infestions in the international timber trade, in the assembly and the use of infested timber and, in all cases, to be able to carry out selective, targeted and localised treatments and to verify their success.

1. Introduction

The degradation of structural timber by attacks of xylophagous insects is a global problem that is partly unavoidable as wood is sensitive to the laws of survival inherent to the nature from which it originates. Under certain conditions, the risk of attack by decay fungi and different kinds of insects can be high. Preventive and curative treatments, once the attack has already occurred, cause enormous economic costs worldwide.

Hylotrupes bajulus L. (house longhorn beetle) is a species of European origin that has spread throughout most of the world [35]. Its larvae are polyphagous and can live and feed on many types of wood with low moisture content, where they can remain for several years until they reach the development necessary to pupate. They generally live in coniferous woods of genera such as *Pinus, Abies* and *Picea*, although they have also been reported on *Populus, Quercus, Acacia, Salix*, etc. [35]. Due

to its ability to attack almost any type of wood and its resistance, it is the cerambycid that can cause the greatest damage to structural wood, carpentry and furniture and has been extensively studied in most treatises on insect pests [5,36,28,8,7]. Its larvae lodge inside the wood, usually at a shallow depth, and move very slowly. For this reason, visual inspection systems have traditionally been used to detect them, based on the location and identification of the detritus and the exit holes of the adult insect; careful listening to the sound made by its specimens when biting the wood, which requires considerable expertise and is subject to subjectivity and the influence of background noise; and others based on more or less complex instrumentation.

Acoustic emissions (AE) are elastic waves in solid materials caused by fractures in macro- or microstructures or by friction, used routinely as a standard method to study fatigue and other phenomena in materials engineering. In wood, the possibility of recording sounds or recording AE with the aim of identifying active insect attack has long been

published [25,24,10] and in recent years has received renewed attention [23] incorporating signal analysis and artificial intelligence [2]. Plinke [26] have published recent advances in the measurement and evaluation of emitted acoustic signals, with some limitations regarding the placement of the sensors, which must be in firm contact with the wood, and the temporary inactivity of the larvae. Commercial "remote sensing" applications are also becoming available [27]. Current methods focus on detection, but do not provide information on larvae location. In contrast, there are numerous works on acoustic geolocation of terrestrial higher animals such as elephants, wolves and marine animals such as whales [6,22,14]. The aim of this work has been to find and develop a low-cost, non-contact technique, using a MEMS microphone array, capable of detecting and accurately locating active house longhorn beetle larvae inside wood. The system is aimed at controlling infections in museums and other places where the protection of heritage wood is needed, unintentional infections in the international timber trade, in the assembly and use of infected wood, and, in all cases, it allows for the execution of selective, targeted and localized treatments and the verification of their success.

2. Description of the acquisition system (AIF)

The acquisition system used consists of 3 elements: 1) an acoustic array of MEMS microphones; 2) an acquisition and pre-processing system based on FPGA/Processor and 3) a PC-based analysis, detection and visualisation application. All software developed on the different platforms is original and has been done using the LabVIEW 2021 programming language. A block diagram of this acquisition and preprocessing system is shown in Fig. 1.

2.1. Acoustic array

An array is an arranged set of identical sensors working in a coordinated manner [33]. In this case, microphone arrays, working together with beamforming techniques [34], allow the localisation of acoustic sources [32,9,37].

The acoustic array used in this work consists of digital MEMS microphones. The acronym MEMS (Micro-Electro-Mechanical Systems) refers to mechanical systems with a dimension of less than 1 mm [12] in the field of integrated circuits (ICs). In the case of MEMS microphones, each of the chips that make them up includes a microphone, a signal conditioner and an acquisition device [1]. These characteristics of these sensors make it possible to have acoustic arrays with a large number of channels, at a reduced cost and size.

2.1.1. Nearfield beamforming

Assuming a plane wave $x(t)$ with a direction of arrival θ, and a linear array with N sensors separated a distance d, the signal received at each sensor x_n, is a phase-shifted replica of $x(t)$. A beamformer combines linearly the signals x_n, which are previously multiplied by complex weights w_n, obtaining an output signal $y(t)$. Fig. 2, shows the general structure of a beamformer.

Using the appropriate weights allows spatial filtering, giving greater gain to signals arriving from a given direction, called steering angle, over the rest [21,34]. The graphical representation of the spatial response of a beamformer versus the angle or the direction of arrival is called the beampattern. It should be noted that the beampattern is also highly dependent on the position of the sensors within the array, known

Fig. 1. Block diagram of the acquisition and pre-processing system.

as array geometry.

Beamformers can be classified as data independent or as statistically optimum, depending on the weights selection [34]. The weights in a data independent beamformer, which has been used in this work, do not depend on the array data and are chosen to show a specified response for all working scenarios. The simplest data-independent beamformer is the Delay-and-Sum beamformer [3], which applies time delays to the signals obtained by the array sensors to compensate for delays in the arrival of the signal of interest at each array sensor due to the signal propagation itself. In this way, the signals are aligned in time and subsequently summed, forming a single output signal $y(t)$, as shown in Fig. 3. The Delay-and-Sum beamformer corresponds, for the general beamformer shown in Fig. 2, to the specific case of using w_n weights of amplitude 1 and phases equivalent to the delays associated with each of the sensors.

The classical delay and sum beamformer is based on the consideration that the source of the signal to be detected is far enough away from the array to assume a far-field situation, so that the delay with which the signal reaches each sensor in the array depends only on the position of the sensor and the pointing angle. Despite this fact, it should be noted that in the system presented in this study these far-field conditions are not met, but it is possible to use the considerations of the delay and sum conformer in near-field conditions [13,4,11], as is the case. In near-field conditions, what must be taken into consideration is that the associated time delays also depend on the relative distance from the emitter to each sensor in the array, as a spherical propagation of the signal must be assumed, as can be observed in Fig. 4.

Since in this case the plane where the sounds (the larvae emissions) are originated is known, the exact delay associated to the propagation of the signal between each of the grid points defined in the analysis/emission plane and each sensor of the array can be determined and used in the delay and sum algorithm. So, the array output in this case can be expressed by

$$y(\overrightarrow{r_g}, t) = \frac{1}{M} \sum_{n=1}^{N} w_n \cdot x_n \left(t - \tau_n\left(\overrightarrow{r_g}\right) \right)$$

where $\overrightarrow{r_g}$ represents the distance of the reference point to one of the focused points defined by the grid. The reference point is arbitrarily defined. In the specific case shown in Fig. 4, is the first sensor on the left of the array. As it was indicated in Fig. 2, N is the number of the sensors, w_n is the weight applied to the n channel of the array (which is equal to 1, as a delay and sum beamformer has been used), and $x_n(t)$ represents the signal acquired by sensor n of the array. $\tau_n(\overrightarrow{r_g})$ indicates the individual time delay of sensor n of the array to the reference point, considering that the signal is a spherical wave, and it is obtained by

$$\tau_n\left(\overrightarrow{r_g}\right) = \frac{\left|\overrightarrow{r_g}\right| - \left|\overrightarrow{r_g} - \overrightarrow{r_n}\right|}{v_{sound}}$$

where $\overrightarrow{r_n}$ represents the distances of the reference point to sensor n of the array.

2.1.2. Array performance

In this study, a planar array has been used, with its elements distributed on a completely flat surface. In the case of a linear array, one direction of arrival can be discriminated, whereas using a two-dimensional, or planar, array two-dimensional information on the location of acoustic sources, which in this case are none other than the larvae, can be obtained, as the corresponding array response is a 2D beampattern. Specifically, this array consists of 486 SPH0641LU4H-1 digital MEMS microphones of Knowles [30], and has a spatial aperture of about 35 cm, in both spatial dimensions.

The angular resolution of the 2D array used depends basically on the working frequency and the pointing angle, as shown in Fig. 5. In this figure it can be observed that the beamwidth decreases as the analysis frequency of the acoustic emissions increases. It can also be noted that
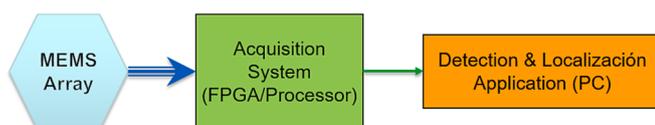
Fig. 2. Structure of a beamformer.

$$* \tau = \frac{d \cdot sin\theta}{v_{sound}}$$

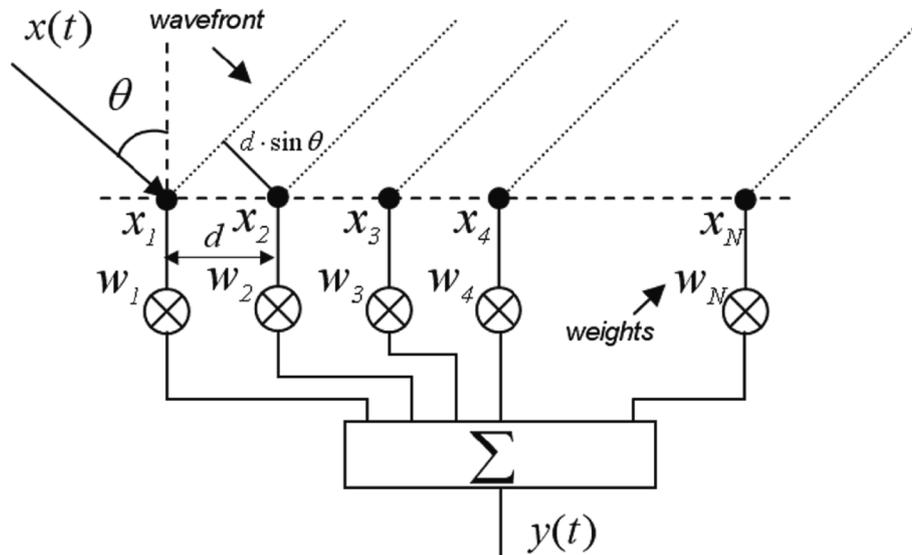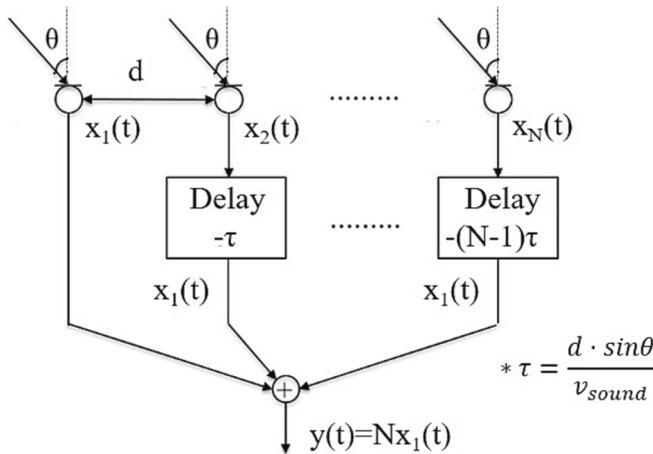**Fig. 3.** Delay and Sum beamformer.

the beamwidth widens as the pointing angle increases from the boresight, i.e., pointing at 0°, to the maximum pointing excursion of 50° defined for this study. The smaller the beamwidth the better the angular resolution and the more accurately the position of the larvae on the beams under test, as well as the position of two larvae in close proximity, can be determined.

Establishing a maximum angular resolution of 10°, and a maximum angular excursion of 50° for the acoustic beams, it can be inferred that the minimum working frequency must be higher than 12 kHz. Specifically, working in the 12 kHz to 24 kHz frequency band, the beamwidths vary between 2.6° and 10°. For practical purposes, the frequency band of interest has been reduced to the range between 13 kHz and 23 kHz to allow proper implementation of the necessary digital bandpass filters.

In previous works reviewed, related to roundheaded wood borer larvae [16,15,31,19], the corresponding acoustic emissions were characterized in bands with maximum frequencies of 10 kHz, typically using piezoelectric sensors and accelerometers in contact with the piece of wood under analysis. But there are also works [18,31] that describe the usefulness of the ultrasonic band. Therefore, the use of this new working frequency band allows exploring its potential for detection and for localization using acoustic arrays. Specifically, the chosen working band: i) takes advantage of the frequency response of MEMS microphones that have a high sensitivity to high frequencies [30], and ii)

reduces the contribution of ambient noise by discarding low frequencies [18].

2.2. Acquisition and processing system

The base unit of the acquisition system is an sbRIO 9607 platform [29]. This platform belongs to National Instruments, particularly to the Reconfigurable Input-Output (RIO) family of devices. Specifically, this sbRIO platform is an embedded single-board controller, running NI Linux Real-Time with an FPGA Zynq-7020 and a dual-Core 667 MHz processor. The FPGA has 96 digital inputs/outputs, of which 81 are used as the connection interface with 162 MEMS microphones of the array, so that in each I/O line, two microphones are multiplexed, while the other lines are used to generate the clock and synchronise. The processor is equipped with 512 MB of DDR3 RAM, 512 MB of built-in storage space, USB Host port, and Giga Ethernet port. Specifically, 3 interconnected cards have been used to guarantee the synchronous capture of the 486 sensors of the used array.

2.3. Analysis, localisation and visualisation software

Based on a Personal Computer and in LabVIEW 2021 programming language, specific software has been developed that handles the following tasks:

- Control of the capture operations of the 3 acquisition cards in a synchronised manner.
- Detection of larvae activity on a continuous basis.
- Storage of the detected signals for further segmentation to isolate the short duration sounds (typically 1–2 ms) produced by the larvae when biting wood.
- Implementation of beamforming algorithms to localise the position of the detected sounds.
- Finally, implementation of a control interface to display a 2D image with the localised positions over an established time frame.

3. Test setup

This section describes the setup of the measurement system inside an anechoic chamber which is based on an extensive array of MEMS microphones. It also describes the setup of the wooden beams and how 6 larvae have been implanted. Finally, a temporal and frequency characterisation of the captured signals is given.
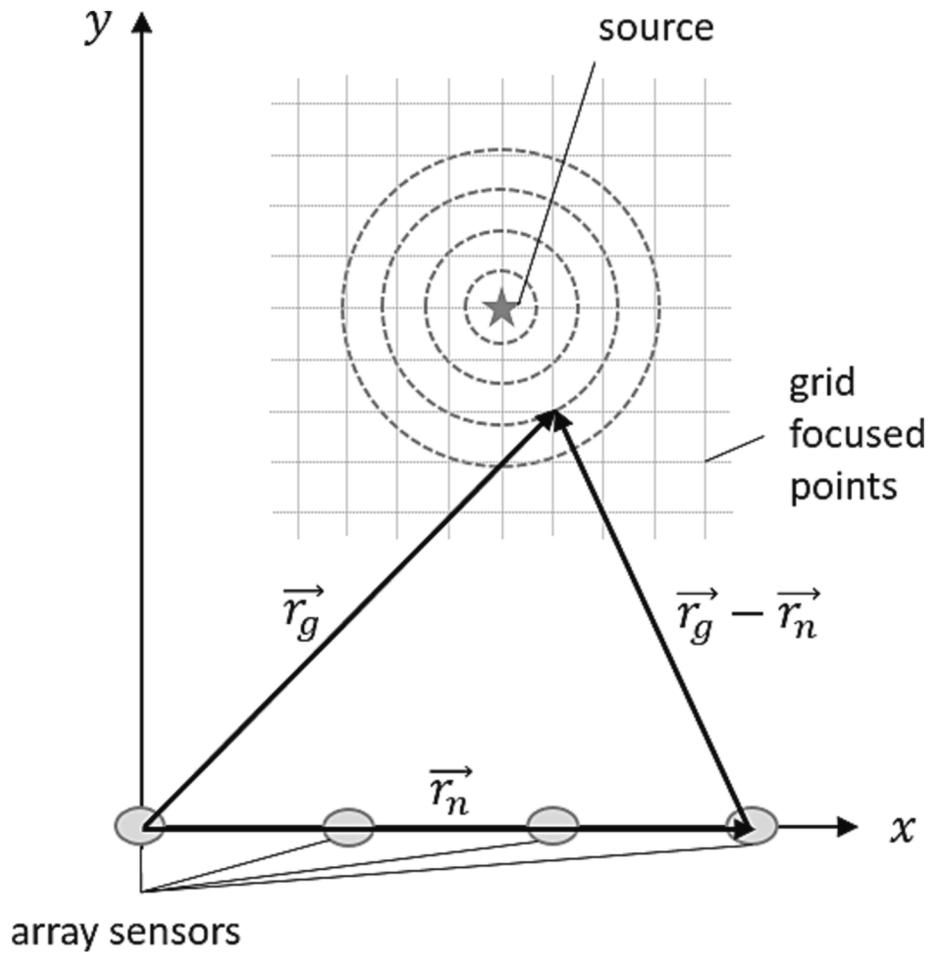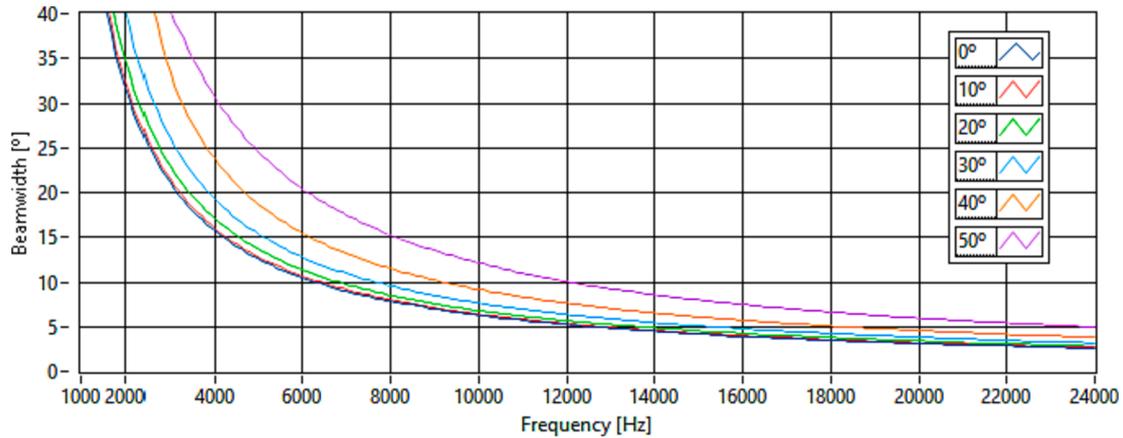
Fig. 4. Nearfield considerations.

Fig. 5. Array beamwidth vs. Working frequency and pointing angle.

3.1. Test set-up

6 larvae of *Hylotrupes bajulus* L. weighing between 0.22 g and 0.35 g were implanted in 4 pieces of wood measuring 90x140x1200 mm of Scots pine (*Pinus sylvestris* L.), previously conditioned to a moisture content of 12%. The larvae were extracted from demolished wood from historical buildings in the city of Valladolid, Spain.

To implant the larvae, a hole was made in the opposite side of each piece of wood, so that the end of the hole was 10 mm from the sapwood observation side. The larva is placed at the end of the hole and the hole is sealed with tissue paper. The larvae are distributed in such a way that different phenomena of sound propagation in wood, edge effect, etc. can be studied.

Once the larvae have been implanted in the wooden specimens, the initial position of the larvae is marked on the corresponding wooden parts with a yellow sticker, and the wooden specimens are placed in a frame to facilitate their simultaneous study (Fig. 6). This set-up makes it possible to simulate the presence of several simultaneous infestations. The larvae are allowed to acclimatise for 30 days. After this time the listening tests are started.
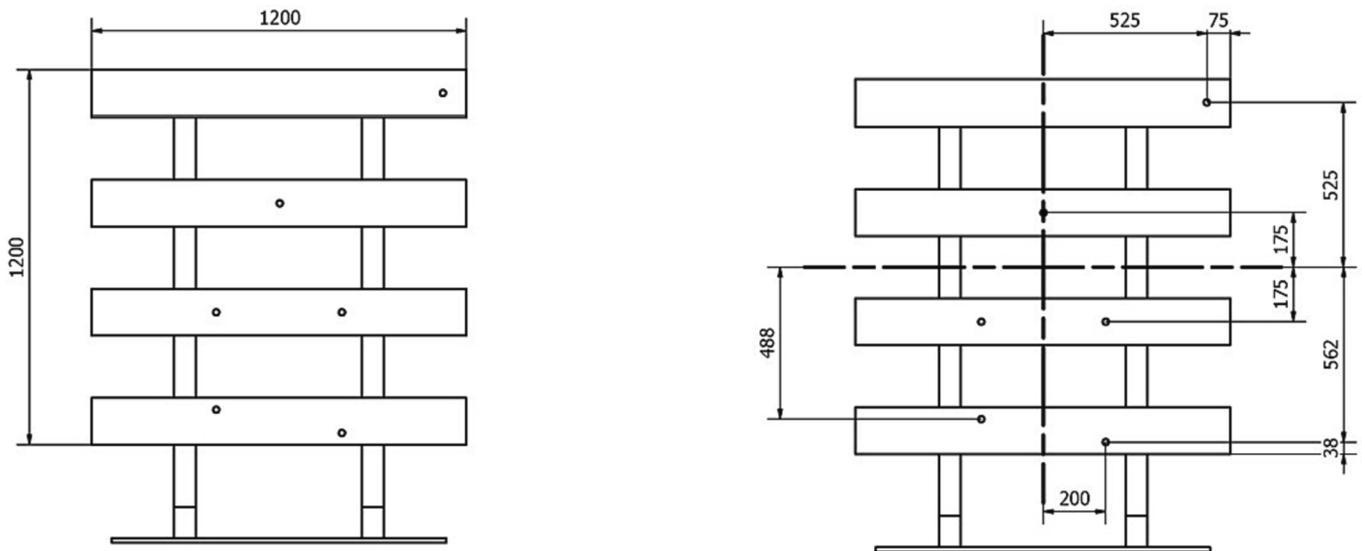
Fig. 6. Location of the 6 larvae within the wooden frame. Distances in mm.

The test setup is implemented inside an anechoic chamber, placing the listening system, i.e., the MEMS microphone array, parallel to the frame, centred with respect to the wooden parts, and 600 mm apart (Fig. 7). The environmental conditions in the anechoic chamber were approximately 24 °C and 40 % RH. Fig. 8 shows an image of the set-up implemented for the tests.

To check the final location of the larvae, a manual milling machine was used to remove the larvae.

3.2. Time and frequency characterisation

Based on the signals analysed during the acquisition phase, where more than 50,000 detections generated by the 6 larvae were obtained, their duration and spectrum were characterised. Traditionally, acoustic detection systems work in the band between 80 Hz and 8000 Hz [19] and can even go up to 10 kHz [17] due to the limited bandwidth of the accelerometers used and the low sensitivity of microphones at higher frequencies.

In the acquisition system used, based on an array of MEMS microphones, it must be considered that the overall sensitivity of the system is very high due to having hundreds of microphones working together and that the angular resolution, which is necessary to locate the position of the larvae accurately, improves as the working frequency gets higher.

The array used allows angular resolutions of between 4^0 and 8^0 depending on the working frequencies. On the other hand, this array has a gain of 26 dB, which allows the remote detection and localisation of very weak acoustic signals, such as those generated by *Hylotrupes bajulus* L. larvae.

The signals emitted by the larvae have a typical duration of 1 ms. Fig. 9a shows a time-lapse realisation of one of these captures. On the other hand, Fig. 9b shows the corresponding average spectrum of the
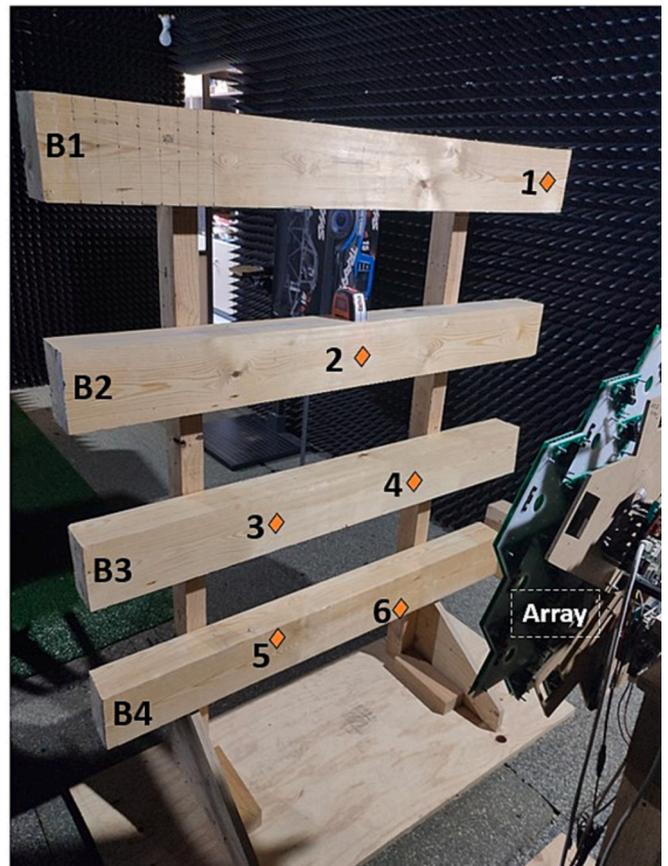

Fig. 8. Image of the setup used. B#: beam. n°: Initial position of larva n.

emitted signals in the defined working frequency band. Based on this information, a band-pass filter will be applied to the signals and a segmentation will be performed as detailed in later sections.

4. Processing algorithm

As functionally described, the implemented processing algorithm consists of the chain of sub-algorithms illustrated in Fig. 10 and
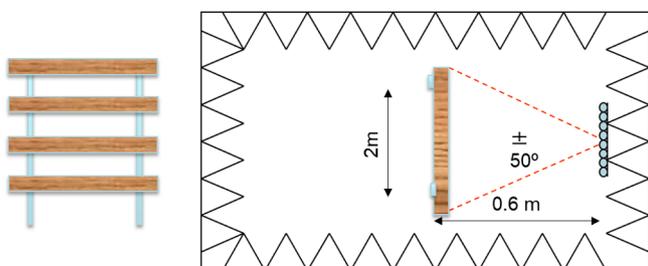

Fig. 7. Test set-up inside the anechoic chamber.
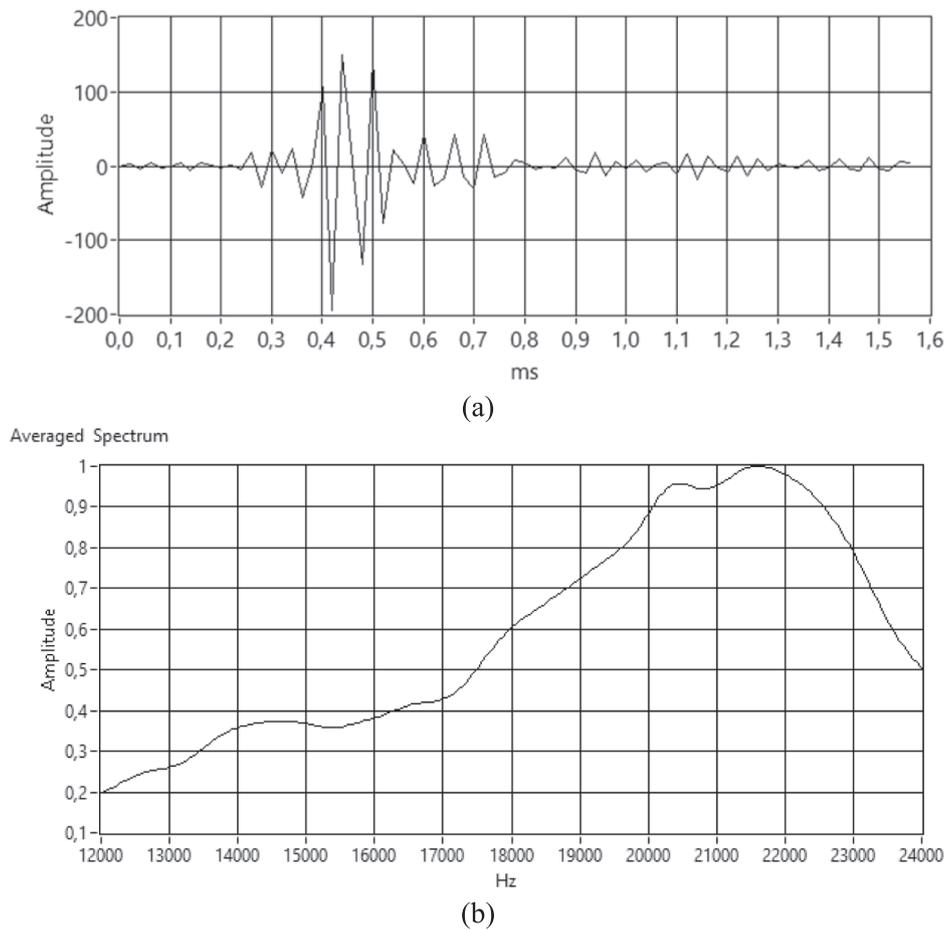
(a)

(b)

Fig. 9. a) Captured filtered time signal. b) Averaged spectrum.

described below.

The acquisition system operates continuously, capturing N samples of a signal x_k of 22.5 ms duration with a sampling frequency fs of 50 kHz, for each of the K sensors that make up the array. A digital anti-aliasing filter with an equivalent cut-off frequency of 24.5 kHz has been included. An example of the K acquired signals can be observed in Fig. 10a.

$$x_k[n] = x_k(nT), T = 1/f_s, n = 0 \cdots N - 1, k = 0 \cdots K - 1$$

First, each of the captured signals is filtered by a digital bandpass FIR filter ($h[n]$), with a passband between 13 kHz and 23 kHz, with a transition band of 500 Hz, designed from the window technique, making use of a Hamming window. The K filtered signals of the example are shown in Fig. 10b.

$$y_k[n] = x_k[n]*h[n]$$

The next step is to detect whether there is activity of any of the larvae in the captured signal. To do this, the sliding energy $E_k[n]$ is calculated over a window of 2 ms for each of the filtered signals using the localised energy technique. The average of the energy estimators $E_k[n]$ is then calculated, as shown in Fig. 10c.

$$E_k[n] = \sum_{r=0}^{N-1} y_k[r]^2 \cdot w[r - n]^2, w[n] = 10 \le n \le M - 1, M = \frac{2 \cdot 10^{-3}s}{T}$$

$$E_{mean}[n] = mean\{E_k[n]\}$$

The estimator $E_{mean}[n]$, is compared with a threshold and in case it exceeds it, the position of the first maximum of the energy n_o is searched for a segmentation. The threshold value is selected so that the system does not detect ambient noise in the test room. In the tests it is assumed

that only one larva is active. If there were several active larvae during the 25 ms captures, E_{mean} would show several maxima. In this case, it would be necessary to select only one of the maxima for the subsequent shaping algorithm to correctly identify the position of a larva.

$$n_0 = \min\{n\}|E[n] \ge threshold$$

In the segmentation, for each of the 25 ms $y_k[n]$ filtered signals, a segment of 2 ms duration is extracted, indexed by n_o, so that it contains the acoustic signal emitted by the larva. The corresponding segmented signals are shown in Fig. 10d.

$$z_k[n] = y_k[n - n_0] \cdot w[n], w[n] = 10 \le n \le M - 1, M = \frac{2 \cdot 10^{-3}s}{T}$$

Using beamforming techniques, and specifically the Delay and Sum algorithm adapted to nearfield conditions, an acoustic image is constructed from the generation of $L_1 \times L_2$ shaped beams to analyse the corresponding spatial positions in the plane containing the 4 wooden beams under analysis. The plane to be analysed, which is the one where the larvae are, is divided into L_1 positions in the horizontal coordinate and L_2 positions in the vertical coordinate, and each of the shaped beam points to each of the $L_1 x L_2$ intersections, as shown in Fig. 11. In the experiment carried out, this plane has dimensions of 120×120 cm, and is analysed with a resolution of 2 cm in both coordinates, so that a total of 61x61 beams were generated.

$$B_{i,j}[n] = Delay\&Sum\{z_k[n]\}, 0 \le i \le L_1 - 1, 0 \le j \le L_2 - 1$$

Finally, the energy of the shaped beams is calculated and plotted, forming an acoustic image of the analysis plane containing the 4 wooden beams. The corresponding acoustic image of the example can be seen in
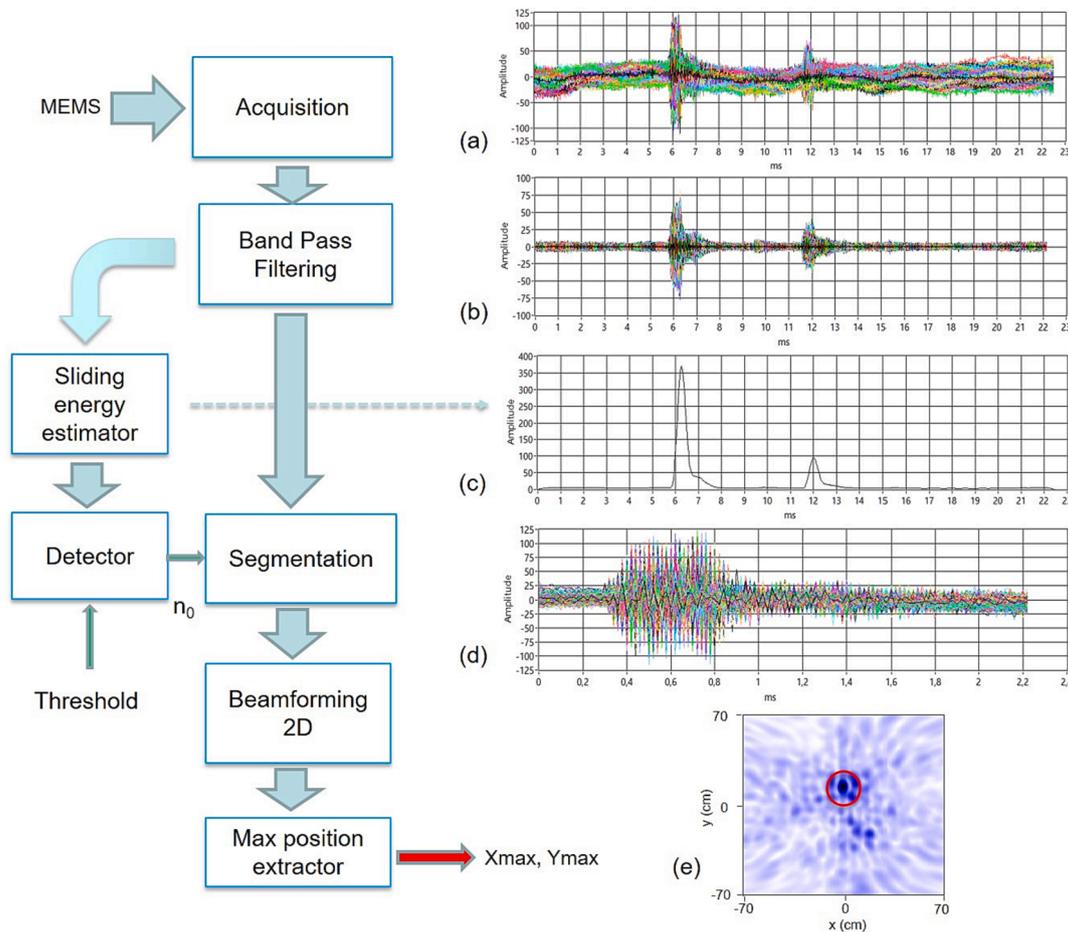
Fig. 10. Processing steps and corresponding signals.

Fig. 10e.

$$E[i,j] = \sum_n \left(B_{i,j}[n] \right)^2$$

From the acoustic image, the coordinates of the maximum of the image are obtained (X_{max}, Y_{max}), which would correspond to the position detected for the larva.

5. Analysis of results

After acquiring about 2.5 million captures, over a period of 2 months, 50,000 captures were obtained in which there was activity of the implanted larvae, which is 2% of the number of captures. In this section we will first analyse the acoustic images obtained based on the algorithm described in Section 4. Then we will verify the behaviour of the larvae and the extent of the galleries drilled during the analysis period.

5.1. Acoustic image analysis

For the analysis of the larvae positions, a 2D histogram has been made with the positions of the maximum of each of the 50,000 acoustic images, as can be observed in Fig. 12. In this 2D histogram, in addition, the initial positions of the 6 larvae have been marked with a green cross. The boundaries of each of the 4 wooden beams under analysis are also marked by brown dashed lines. To calculate the histogram, the number of times the position of the maximum (X_{max}, Y_{max}) fell into one of the 61x61 defined cells (Fig. 11) was counted. The values have been normalised and fitted to a colour map on the Z-axis. There are 7 zones where the maximums of the acoustic images are concentrated, with variable

dispersions for each of the larvae since the activity of each of them during the period of analysis and their movements have been variable.

At this point, it should be pointed out that the sound produced by each larva has complex propagation mechanisms, due to the fact that wood is not a homogeneous medium, and the larvae produce internal galleries, so that the sound is generated at one point and then comes out to the surface of the beam through another point, which is experimentally proven to be close to the internal position where it was generated. In addition, there are knots and cracks in the beams that can also alter the exit point of the sound. It is therefore clear that the sound exit points are close to the position where the larvae are located, but that if there are significant fibre deviations, knots or cracks in the beams, the sound will also exit through them. A visual inspection is required to rule out a sound emission zone if there is a band or knot in its proximity and therefore that the remaining detected zones clearly identify the position of the larvae inside them.

5.2. Verification of larvae trajectories inside the wooden beams

All larvae survived implantation and during the 2-month period made tunnels from 110 mm to 290 mm in length (Fig. 13a). This shows that, despite the low moisture content of the wood, their activity was intense.

The wood anisotropy, differences in density between spring and summer wood, together with the presence of anomalies such as knots, cracks, etc. produce refraction and reflection phenomena so that the sound does not always radiate through the area of the wood face closest to the bite. This results in greater uncertainty in locating the larvae. Fig. 13b shows the image generated by the array with the actual
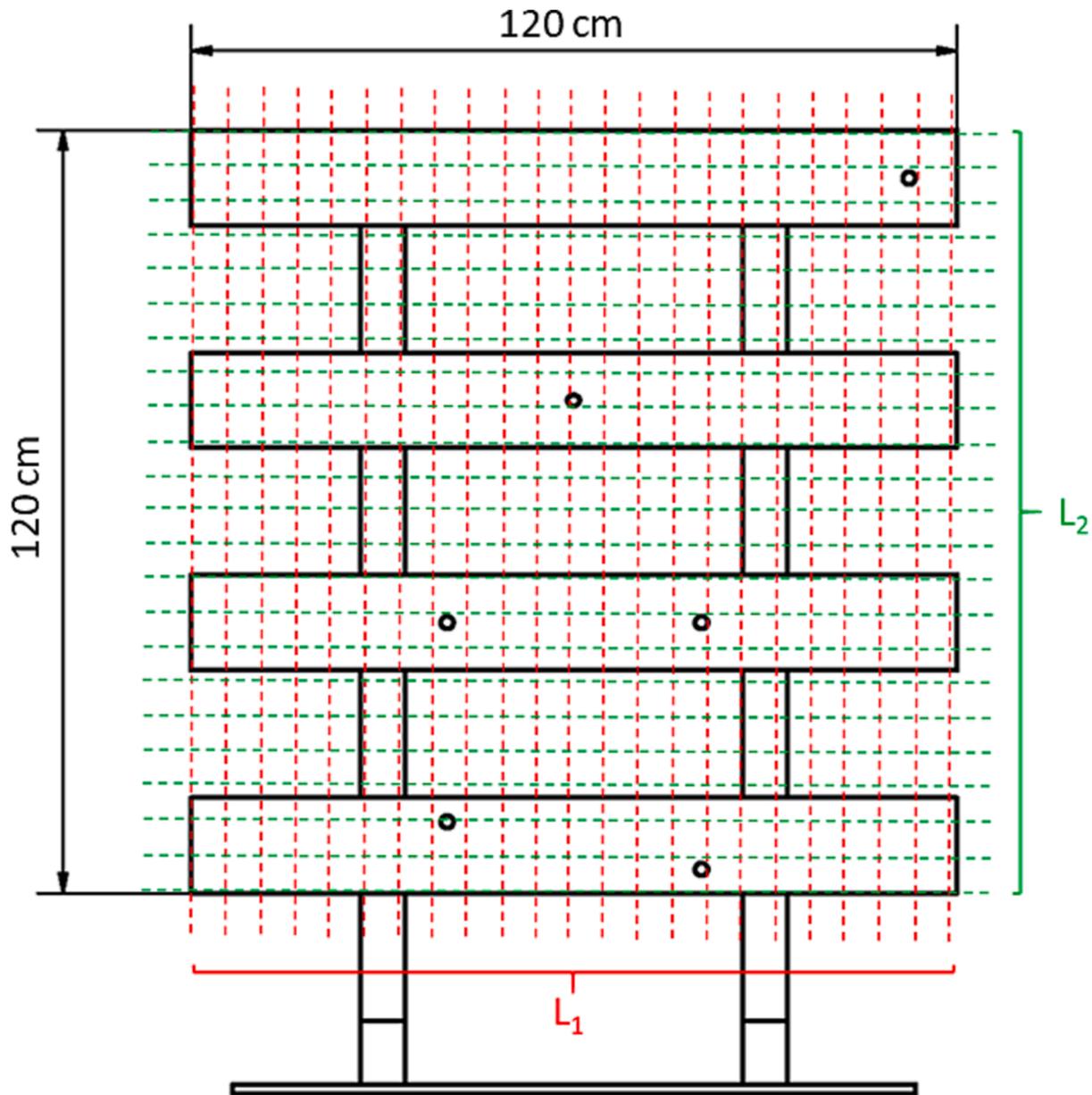
Fig. 11. Assessment positions for beamforming.

positions of each of the 6 larvae and the location obtained by the system, together with the level of energy received.

In the case of larva 1, it can be observed that there is a focus of sound emission to the left of the actual position of the larva. At this point, there is a fibre deflection due to a set of inclusive knots. This fibre deflection causes the growth rings being gnawed by the larva to surface. The speed of sound propagation is around 4 times higher, and the attenuation is lower in the fibre direction than in the perpendicular direction [20]. As can be observed in Fig. 14, if the fibre bundle being eaten by the larva is lengthened, there is a deflection of fibres such that the fibres emerge at the surface close to a knot. This deflection of fibres acts as a conduit for better sound propagation. Next to larva 1 there is another more concentrated and more energetic detection focus that allows the larva to be located.

In the case of larvae 2 and 5, the device located the larvae in the air gap immediately below or above the wooden beams respectively. This is explained by the fact that the larvae were located on the side perpendicular to the observation face.

Larvae 3, 4 and 6 are correctly located by the equipment.

6. Conclusions

A non-contact low-cost acoustic system, based on a low-cost MEMS microphone array, sensitive to the acoustic signals produced by cerambycid larvae when they tear wood to feed, allowing the detection and actual localisation of multiple individuals inside structural-sized pieces of wood, has been developed.

The work indicates that different anomalies in the wood, mainly cracks and knots, can cause the focus of the sound output and the place where the larva generates it to be distant. This results in failures in larvae localization or a splitting of the localization. In any case, the error in the localisation is inside the wood internode, which can be considered as the minimum unit of anti-xylophagous treatment. Therefore, the system presented can be used to carry out specific treatments as opposed to the extensive treatments currently used.

Bearing in mind that the growth of larvae is not linear, since the larger they are the more they can grow, and that when they hatch they are so small that they cannot be heard, a future line of research associated with this work could focus on the study of the influence of larva size
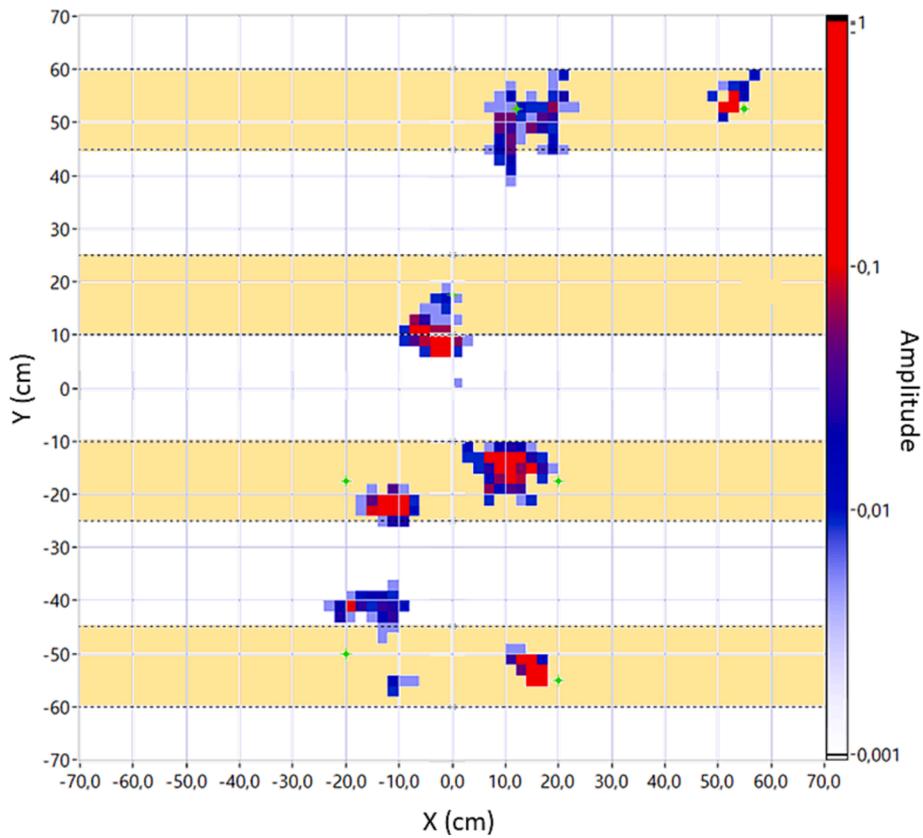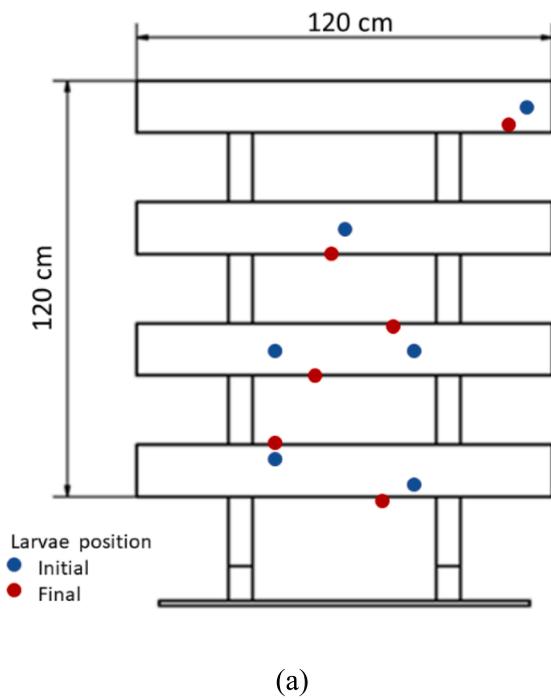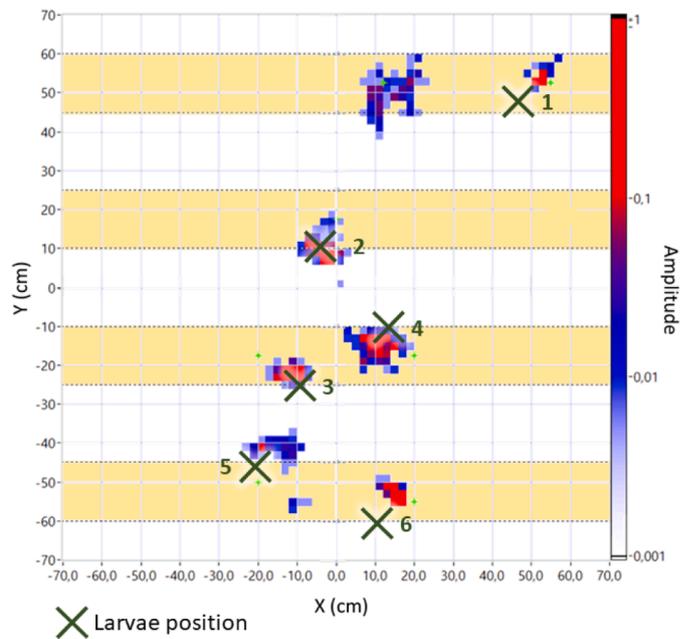
Fig. 12. 2D histogram with estimated larvae positions from acoustic images.

(a)

(b)

Fig. 13. (a) Initial and final position of each of the larvae. (b) Location by the system and actual position of the larvae.

on the system's detection capacity, or on how larva size influences the detection threshold to be defined for the system.

The study could also be extended to the detection of the feeding patterns and the galleries of other xylophagous organisms, such as common woodworm or termites. Field tests could also be conducted to evaluate their performance outside the laboratory environment. In the future, the system could address the identification of the specific type of xylophage responsible for the deterioration by using machine learning
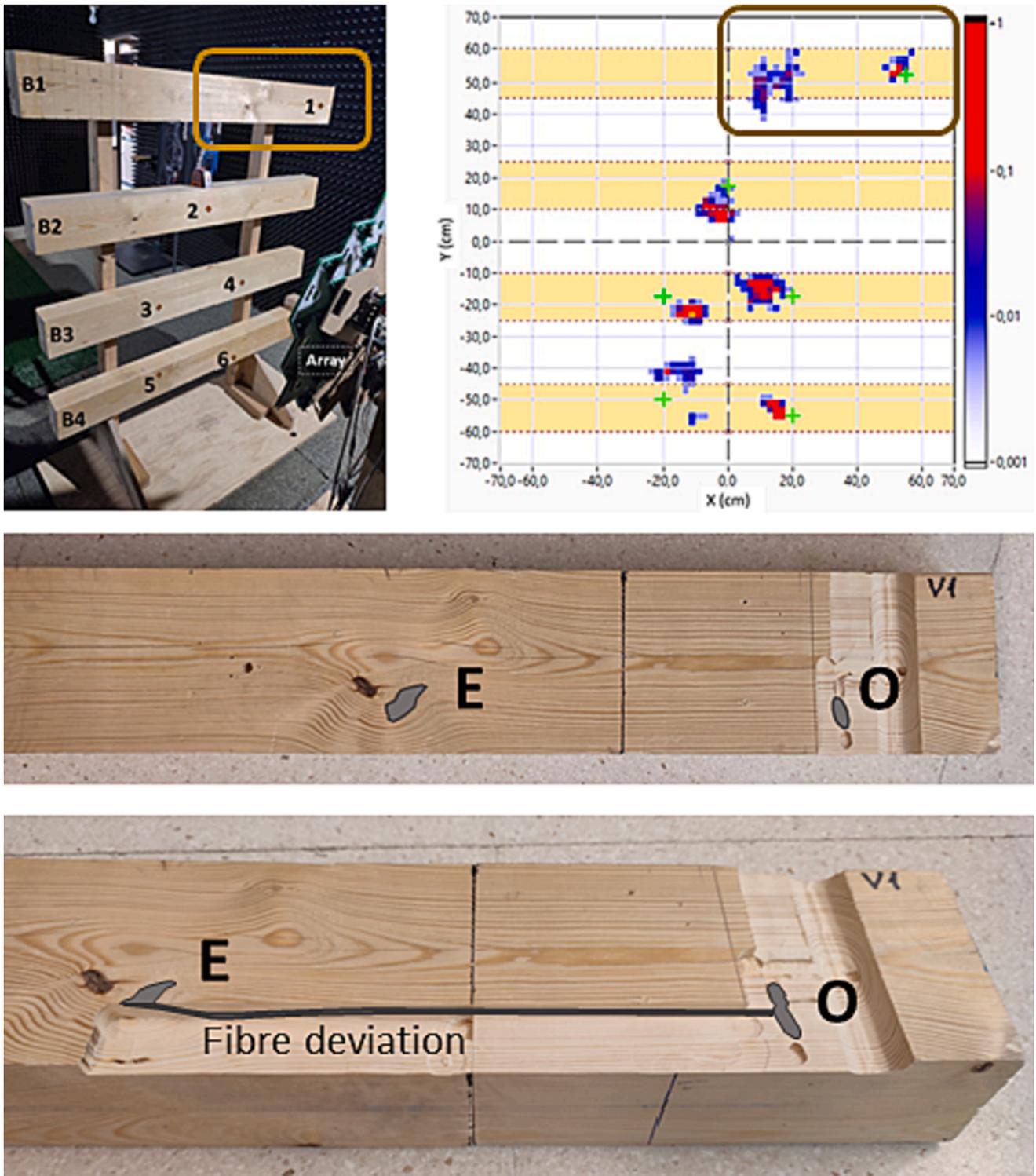
Fig. 14. Simultaneous foci of sound emission from larva 1 due to fibre deflection. O: origin of sound generated by larvae chewing, E: secondary output of sound.

or equivalent techniques, based on the temporal and frequency information of the detected sound events. This would allow for even more targeted and localised curative treatments.

CRediT authorship contribution statement

Roberto D. Martínez: Conceptualization, Methodology, Writing – original draft, Writing – review & editing. **Alberto Izquierdo:** Conceptualization, Methodology, Investigation, Data curation, Writing – original draft. **Juan José Villacorta:** Methodology, Investigation, Data curation. **Lara del Val:** Investigation, Writing – original draft, Writing – review & editing. **Luis-Alfonso Basterra:** Conceptualization, Writing – original draft, Writing – review & editing.

Declaration of Competing Interest

The authors declare that they have no known competing financial interests or personal relationships that could have appeared to influence

the work reported in this paper.

Data availability

Data will be made available on request.

Acknowledgments

References

[1] Beeby S, Ensell G, Kraft M, White N. MEMS Mechanical Sensors. In: House A, editor. Publishers. Norwood: Artech House Publishers; 2004.

[2] Bilski P, Bobiński P, Krajewski A, Witomski P. Detection of Wood Boring Insects' Larvae Based on the Acoustic Signal Analysis and the Artificial Intelligence Algorithm. Arch Acoust 2016;42(1):61–70. https://doi.org/10.1515/AOA-2017-0007.

[3] Brandstein, M.; Ward, D. Microphone Arrays; Springer: New York, NY, USA, 2001.

[4] Cho Y.T.; Roan M.J., "Adaptive near-field beamforming techniques for sound source imaging", in J Acoust Soc Am 125, 944–957 (2009). https://doi.org/10.1121/1.3050248.

[5] Demelt, C. 1966. Die Tierwelt Deutschlands, II. Bockkäfer Oder Cerambycidae. I Biologíe Mitteleuropäischer Bockkäfer Unter Besonder Berücksichtigun Der Larven. Vol. II. Jena: G. Fischer.

[6] Dissanayake CM, Kotagiri R, Halgamuge MN, Moran B. Improving Accuracy of Elephant Localization Using Sound Probes. Appl Acoust 2018;129(January):92–103. https://doi.org/10.1016/j.apacoust.2017.07.007.

[7] Duffy EAJ. A Monograph of the Immature Stages of British and Imported Timber Beetles (Cerambycidae). London: British Museum (National History); 1953.

[8] Duffy EAJ. A Monograph of the Immature Stages of African Timber Beetles (Cerambycidae). London: British Museum (National History); 1957.

[9] Edstrand, A, C. Bahr, M. Williams, J. Meloy, T. Reagan, D. Wetzel, M. Sheplak, and L. Cattafesta. 2011. "An Aeroacoustic Microelectromechanical Systems (MEMS) Phased Microphone Array." In *Proceedings of the 21st AIAA Aerodynamic Decelerator Systems Technology Conference and Seminar*. Dublin.

[10] Fujii, Y, M Noguchi, Y Imamura, and M Tokoro. 1989. "Detection of Termite Attack in Wood Using Acoustic Emissions." In *Proceedings IRG Annual Meeting*. Lappeenranta.

[11] He T, Pan Q, Liu Y, Liu X, Hu D. Near-field beamforming analysis for acoustic emission source localization. Ultrasonics 2012;52(5):587–92. https://doi.org/10.1016/j.ultras.2011.12.003.

[12] Hsieh, C.T, J.-M. Ting, C. Yang, and C.K. Chung. 2002. "The Introduction of MEMS Packaging Technology." In *In Proceedings of the 4th International Symposium on Electronic, Materials and Packaging*. Kaohsiung.

[13] Kennedy RA, Abhayapala TD, Ward DB. Broadband nearfield beamforming using a radial beampattern transformation. IEEE Trans Signal Process Aug. 1998;46(8):2147–56. https://doi.org/10.1109/78.705426.

[14] Kershenbaum, Arik, Jessica L. Owens, and Sara Waller. 2019. "Tracking Cryptic Animals Using Acoustic Multilateration: A System for Long-Range Wolf Detection." *The Journal of the Acoustical Society of America* 145 (3): 1619–28. https://doi.org/10.1121/1.5092973.

[15] Mankin, R W, D W Hagstrum, M T Smith, A L Roda, and M T K Kairo. n.d. "Perspective and Promise: A Century of Insect Acoustic Detection and Monitoring." Accessed March 14, 2023. https://academic.oup.com/ae/article/57/1/30/2462094.

[16] Mankin RW, Smith MT, Tropp JM, Atkinson EB, Jong ADY. Detection of Anoplophora Glabripennis (Coleoptera: Cerambycidae) Larvae in Different Host Trees and Tissues by Automated Analyses of Sound-Impulse Frequency and Temporal Patterns. J Econ Entomol 2008;101(3):838–49. https://academic.oup.com/jee/article/101/3/838/806198.

[17] Mankin, R W, A Mizrach, A Hetzroni, S Levsky, Y Nakache, V Soroker. 2008. "Temporal and Spectral features of sounds of Wood-Boring Beetle Larvae: identifiable pattrerns of activity enable improved discrimination from background noise." *Florida Entomologist* 91 (2). https://doi.org/10.1653/0015-4040(2008)91[241:TASFOS]2.0.CO;2.

[18] Mankin RW, Hagstrum DW, Smith MT, Roda AL, Kairo MTK. Perspective and Promise: a Century of Insect Acoustic Detection and Monitoring. Am Entomol 2011;57(1):30–44.

[19] Mankin R, Hagstrum D, Guo M, Eliopoulos P, Njoroge A. Automated Applications of Acoustics for Stored Product Insect Detection, Monitoring, and Management. Insects 2021;12:(3). https://doi.org/10.3390/insects12030259.

[20] Martinez, Roberto, Ignacio Bobadilla, Guillermo Iñiguez, Francisco Arriaga, Miguel Esteban, and Eva Hermoso. 2010. "Assessment of Decay in Existing Timber Members by Means of Wave Velocity Perpendicular to the Grain." In *11th World Conference on Timber Engineering 2010, WCTE 2010*, 1471–75. Riva di Garda.

[21] Naidu, PS. Sensor Array Signal Processing, 1st ed; CRC Press: Boca Raton, FL, USA, 2001.

[22] Noad, Michael J, Douglas H Cato, and M Dale Stokes. 2004. "Acoustic tracking of humpback whales: measuring interactions with the acoustic environment." In *Proceedings of Acoustics*.

[23] Nowakowska M, Krajewski A, Witomski P, Bobiński P. Thermic Limitation of AE Detection Method of Old House Borer Larvae (Hylotrupes bajulus L.) in Wooden Structures. Constr Build Mater 2017;136(April):446–9. https://doi.org/10.1016/J.CONBUILDMAT.2017.01.012.

[24] Pallaske M. Measurement and Analysis of the Activity of Larvae of the House Longhorn Beetle Hylotrupes bajulus (L.) in Wood and in an Artificial Diet with the Aid of Modern Electronics. Material Und Organismen 1986;21(1):63–79.

[25] Pence, Roy J, S J Magasin, and R G Nordberg. 1954. "Detecting Wood-Boring Insects Electronic Device Developed as Aid in Locating Insects Destructive to Timber and Wood Products".

[26] Plinke, Burkhard. 2021. "InsectDetect Aktiver Schadinsekten Im Holzhandel." https://www.fnr.de/ftp/pdf/berichte/22WK412101.pdf.

[27] Potamitis, Ilyas, Iraklis Rigakis, Nicolaos-Alexandros Tatlas, and Stelios Potirakis. 2019. "In-Vivo Vibroacoustic Surveillance of Trees in the Context of the IoT." https://doi.org/10.3390/s19061366.

[28] Ruiz A. Insectos Xilófagos: Cuatro Coleópteros de La Madera Labrada. Boletín de Patología Vegetal y Entomología Agrícola 1942;11:201–39.

[29] "SbRIO-9607 Platform." n.d. Accessed March 14, 2023. https://www.ni.com/docs/en-US/bundle/sbrio-9607-feature/page/overview.html.

[30] "SPH0641LU4H-1 MEMS Microphone" n.d. Accessed March 18, 2023. https://www.knowles.com/docs/default-source/model-downloads/sph0641lu4h-1-revb.pdf.

[31] Sutin A, Yakubovskiy A, Salloum HR, Flynn TJ, Sedunov N, Nadel H. Towards an Automated Acoustic Detection Algorithm for Wood-Boring Beetle Larvae (Coleoptera: Cerambycidae and Buprestidae). J Econ Entomol 2019;112(3):1327–36.

[32] Tiete J, Domínguez F, Silva B, Segers L, Steenhaut K, Touhafi A. SoundCompass: A Distributed MEMS Microphone Array-Based Sensor for Sound Source Localization. Sensors 2014;14(2):1918–49.

[33] Trees, Harry L. Van. 2002. *Optimum Array Processing: Part IV of Detection, Estimation, and Modulation*. Edited by John Wiley & Sons. https://books.google.es/books?id=J5TZDwAAQBAJ&dq=Van+Trees,+H.+Optimum+Array+Processing:+Part+IV+of+Detection,+Estimation+and+Modulation+Theory,+John+Wiley+%26+Sons,+2002.++&lr=&hl=es&source=gbs_navlinks_s.

[34] Veen, Barry D. Van, and Kevin M. Buckley. 1988. "Beamforming: A Versatile Approach to Spatial Filtering." *IEEE ASSP Magazine* 5 (2): 4–24. https://doi.org/10.1109/53.665.

[35] Vives, Eduard. 2000. *Fauna Ibérica, Coleóptera: Cerambycidae*. Vol. 12. Madrid: Museo Nacional de Ciencias Naturales.

[36] Zarco E. Sobre El Hallazgo En Santander de Un Coleóptero Perforador de Las Cubiertas de Plomo de Cables Telefónicos. Boletín de La Real Sociedad Española de Historia Natural 1935;35:143–216.

[37] Zhang X, Song E, Huang JingChang, Liu H, Wang YuePeng, Li B, et al. Acoustic Source Localization via Subspace Based Method Using Small Aperture MEMS Arrays. J Sens 2014;2014:1–14.